SURFACE REFLECTANCE ANGULAR SIGNATURES FROM AIRBORNE POLDER DATA

Marc Leroy[1], François-Marie Bréon[2], and Frédéric Fontanari[1]

1: Laboratoire d'Etudes et de Recherche en Télédétection Spatiale
CNES/LERTS
31055 Toulouse, France

2: Laboratoire de Modélisation du Climat et de l'Environnement
CEA/DSM/LMCE
91191 Gif sur Yvette, France

0- ABSTRACT

Thanks to its optical design, the airborne POLDER instrument allows a multidirectional measurement of a surface target reflectance. During the "La Crau 91" experiment, the radiometer has been flying over a study area of 10x10 km composed of various cultivated fields. The measurements have been projected on the surface on a regular grid of resolution 100 m. For each grid point, up to 50 directional measurements provide a good description of the surface directional signature. These signatures are discussed for a few selected targets representative of the area. The measurements show typical features of the reflectance angular signature, including the "hot spot" and specular reflection.

A simple directional model is then applied to the measurements. It provides, for each of the 10^4 grid points, a *normalized* reflectance corrected for the angular effects, together with two parameters which gives a quantitative assessment of the directional signature. The paper discusses these parameters and the ability of the model to reproduce the measurements. To our knowledge, it is the first time that reflectance angular signature are measured at the regional scale, a key step to the operational processing of POLDER measurements at the global scale.

KEY WORDS: Surface reflectance, airborne measurements, directional model, hot spot, POLDER

1- INTRODUCTION

Optical remote sensing of the surface is a very efficient tool for an assesment of land use, vegetation coverage, vegetation health and primary productivity. However, a number of difficulties make difficult the quantitative use of satellite measurements. A major difficulty results from atmospheric effects on the reflectance, in particular due to aerosol scattering. Another difficulty for the use of spectral reflectances is their anisotropy: A daily coverage of the Earth from a limited number of instruments, such as the AVHRR series, requires the measurements to be acquired at various viewing angles, up to about 60°. The reflectance anisotropy makes impossible the direct comparison of measurements acquired at nadir viewing with those acquired at large viewing angles. On the other hand, the reflectance angular signature may be a new source of information, in addition to the spectral signature, for a quantitative monitoring of the surface.

For these reasons, there has been a large interest in the past years on the reflectance directional signature of natural sufaces, either vegetation or bare soil. Directional effects have been identified on satellite data time series (Gutman, 1987; Roujean et al., 1992a). Directional signature measurements have also been acquired in the field (Kriebel, 1978; Kimes, 1983; Kimes et al., 1985) and in the laboratory (Coulson, 1968). Similarly, several models have been designed to reproduce and predict the observed reflectance signatures (Otterman and Weiss, 1984; Pinty et al., 1989; Verstraete et al., 1990; Roujean et al., 1993). The POLDER instrument, either airborne or spaceborne, (Deschamps et al., 1994) has been designed for the measurement of directional effects on the reflectance. Its concept permits to measure the reflectance of a single surface target from several directions as the instrument goes along its path. POLDER will be launched in 1996 on the Japanese ADEOS platform. An airborne version of the instrument has been flying for several years (Bréon and Deschamps, 1993; Deuzé et al., 1993).

During the "La Crau 90" campaign (Deuzé et al. 1993), a first attempt to derive directional signatures from airborne POLDER data was made. Meaningful directional signatures were derived from the measurements for a number of surface vegetation covers that were typical of the area. However, due to a lack of geometric accuracy in the measurements, only surface targets that were homogeneous on a rather large scale (more than a hundred meters) could be studied in terms of directional signatures. Moreover, even the selected targets showed some unexpected noise. These setbacks were corrected for the following campaign that took place in 1991. This paper presents the La Crau 91 POLDER campaign and an analysis of the measurements in terms of surface directional signature. Thanks to the data improved quality, the analysis can be performed on a large number of surface grid points, which is a large improvement to the limited set of target analyzed previously, and a key step to the global scale that will be studied with spaceborne POLDER.

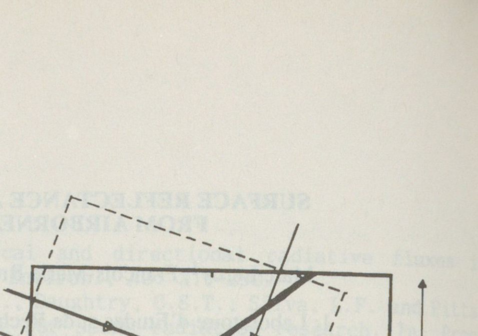

Figure 1: Map of the 10x10km2 study area. The thick lines indicate the flight axis used during the measurements. The dashed line indicates a typical POLDER field of view when the instrument is located at the vertical of the point shown with a cross. The Rhône river and two canals are also shown.

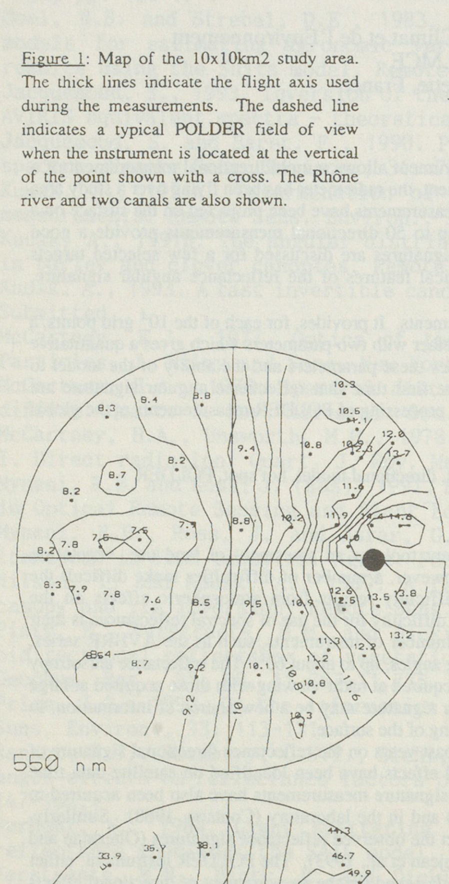

Figure 2: Typical directional reflectance diagram for a sunflower field at 550 nm (top) and 850 nm (bottom). The black circle represents the average zenith angle of the Sun, on the Φ = 0° axis. See text for indications.

2- MEASUREMENT AND PROCESSING

The measurements analyzed in this paper have been acquired during a joint POLDER/AVIRIS campaign that took place in June 1991 (Baret et al., 1992). The area of interest is located in southern France, close to the river Rhone delta, in the so called "La Crau" area. The zone is mostly cultivated with a dominance of rice, wheat and sunflower. Sorghum, grass and orchards are also present. Although the campaign lasted several days, from June 18th to June 24th, June 19th was selected here for its rather low aerosol optical thickness of 0.094 at 550 nm. This value allows us to apply a crude atmospheric correction on the measurements where only single scattering is accounted for.

During the campaign, the POLDER instrument was flown on the ARAT aircraft operated by IGN with a typical flight altitude of 3000 m. The flight pattern is shown in Fig. 1. It is composed of five flight lines parallel to the sun direction , and one perpendicular flight line.

The POLDER instrument optical design is based on the concept of a CCD matrix, a rotating filter wheel that carries spectral filters and polarizers, and a wide field of view lens. On the filter wheel, 9 slots allow 3 spectral measurements, each of them for three polarization directions. During the campaign, the POLDER filter wheel was set up with spectral filters at 550, 650 and 850 nm, each 40 nm wide. The bidimensional CCD matrix permits a view of the area in one instantaneous shot. A typical POLDER field of view is shown in Fig. 1. The POLDER field of view is 51° along track and 43° crosstrack. The field of view on the ground is, therefore, about twice the instrument altitude, or 7.4x5.6 km^2. The CCD matrix is composed of 384x288 pixels, which yields a spatial resolution of about 20 meters. The time lag between two successive shots is 10 seconds which, according to the aircraft flight speed corresponds to 0.7 km. Thus, there is an overlap of 90% between two successive images, and a target on the surface can be seen in 10 POLDER images corresponding to 10 different viewing directions. Similarly, the crosstrack image size is much larger than the distance between the various parallel flight lines. There is, therefore, an overlap between the measurements of those flight lines and a surface target can be observed from the corresponding viewing directions.

Data processing is as follows: The CCD spectral measurements are converted to radiance using calibration coefficients (determined in the laboratory using an integrating sphere) and then to reflectance. A crude atmospheric correction is applied to the measurements:

$$R_{cor} = \frac{R_{mes} - R_{Ray} - R_{aer}}{T_{atm}} \quad (1)$$

where R_{cor} is the reflectance corrected for atmospheric effects, R_{mes} is the measured reflectance, R_{aer} is the estimated aerosol reflectance (according to ground-based measurements of aerosol optical thickness), R_{Ray} is the reflectance resulting from molecular scattering below the aircraft, and T_{atm} is the atmospheric transmitance. In this simple correction, we only account for single scattering and we neglect the coupling between surface reflectance and aerosol scattering. Moreover, we assume the aerosol layer to be homogeneously distributed below the aircraft, and we make use of a theoretical scattering phase function. Although these are strong hypothesis, we have confidence in our corrected reflectances because of the low atmospheric optical thickness. The reflectance presented in this paper are always *corrected* reflectances.

One make then use of the position and orientation parameters given by a GPS system and a gyroscopic central unit connected to the POLDER instrument. Each POLDER image is registered on a surface grid of 10x10 km, shown in Fig. 1, with a spatial resolution of 100 meters. This resolution was chosen because preliminary tests showed that it is the maximal registration error in our measurements. For each grid point, the spectral reflectance is stored together with the solar and viewing angles. The number of directional measurements associated to a given grid point depends on its position in the study area. It reaches a maximum of 50 at the zone center.

3- ANGULAR SIGNATURES OF SELECTED TARGETS

Fig. 2 to 5 are a representation of the reflectance directional signature for selected surface targets. In these polar diagrams, the radius corresponds to the viewing zenith angle. The polar angle is the viewing azimuth relative to the sun direction. The backscattering (azimuth = 0°) is on the right side of the diagram. The polar representations are limited to viewing zenith angles up to 60° since this is the practical limit of airborne POLDER. Each point corresponds to one directional measurement and the figure next to it gives the measured reflectance in percent. The lines are a result of an isocontour processing on the data points. The data points that are aligned in the polar plot correspond to successive measurements of a given flight line.

Visual analysis of the figures gives us confidence in the data quality:

- The successive measurements from a given flight line show a monotonous variation.
- The isolines are relatively symetric with respect to the principal plane (the 0-180° line on the figures). Such symetry is expected if the surface does not have a favoured direction.

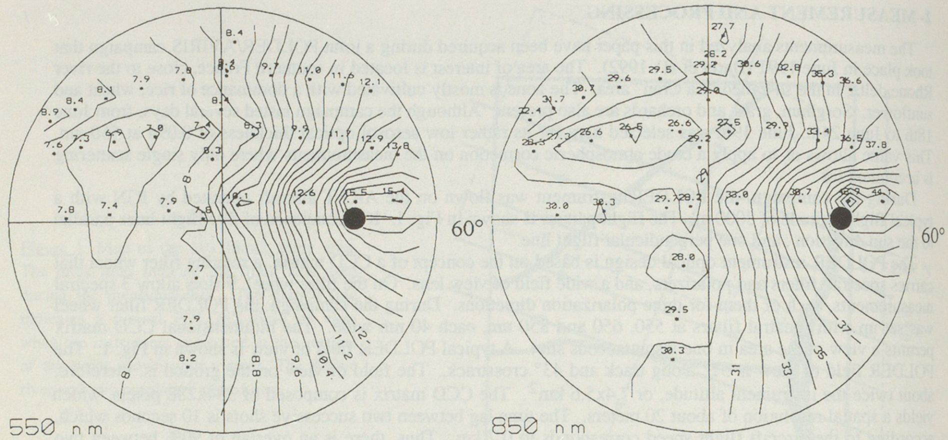

Figure 3: Same as Figure 2 for a wheat field at 550 nm (left) and 850 nm (right).

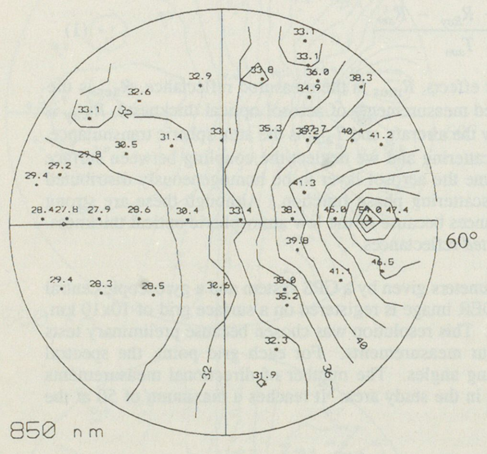

Figure 4: Same as Figure 2 but for a vineyard. Only 850 nm is shown.

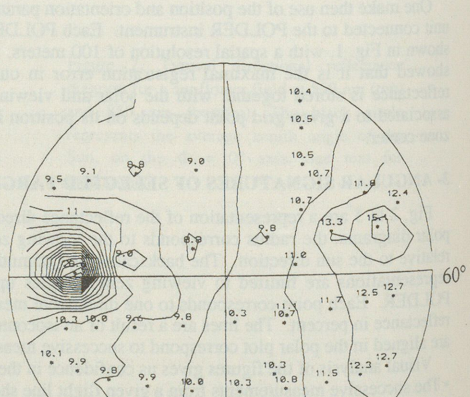

Figure 5: Same as Figure 2 but for a rice paddy. Only 550 nm is shown.

- Two measurements acquired during different flight lines but for similar viewing directions show coherent values. Some differences, which generally do not exceed 5% of relative value, can be explained from the variations in solar zenith angles between the measurements: The flight lasted about 75 mn over our site and the solar zenith angle decreased from 46° to 32°, during that period

Fig. 2 and 3 are the polar representations of the directional reflectance for two dominant cultures of the area, sunflower (Fig. 2) and wheat (Fig. 3) at two wavelengths (550 and 850 nm). The order of magnitude of the reflectance is as expected for vegetation covers: The reflectance in the visible channel is on the order of 10%. It is much larger in the near IR, about 50% for sunflower and 30% for the wheat. The directional signature is consistent with surface measurements: the reflectance generally increases with the viewing angle and it is much larger for backscattering directions than for forward reflection (Kimes, 1983; Kimes et al., 1985). The minimal reflectance is observed in the principal plane, about thirty degrees off nadir, in the forward direction. There is a ratio of about 2 between the maximal and minimal directional reflectance for a given target and spectral band. The observed directional effects can be explained by geometry and shading considerations, as discussed in Kimes (1983).

Another signature of interest, but of limited angular extension, is the "hot spot" in the antispecular direction. In this particular direction, the instrument does not view any shadow and the reflectance is generally maximum. The angular extension of the hot spot depends on the canopy geometry as discussed in Jupp and Strahler (1991). The observation of the hot spot from the surface is difficult since, unless the radiometer is far from the surface, its shadow interfers with the measurement. The airborne POLDER, thanks to its altitude and directional resolution, is able to observe the hot spot. This is partly illustrated in Fig. 4 which corresponds to a vineyard canopy. The largest measurement (R_{cor} = 54 %) is acquired for the direction the closest (θ_v=41°) to the hot spot (principal plane, 38.3° zenith angle). Other measurements closer to the nadir (θ_v=32°), and further from the nadir (θ_v=49°) show a much lower reflectance (45.0 % and 47 % respectively).

Rice fields show a feature that is not observed over other surfaces: a narrow spot of large reflectance (Fig. 5). It results from specular reflectance over flooded areas and affects predominantly the direction symetric to that of the hot spot. In Fig. 5, which corresponds to the 550 nm band, the reflectance is 29% at the specular point, and only 10% a few degrees away. If we do not consider the specular direction measurements, the rice paddies directional signature agrees with that of other surfaces; i.e. a larger reflectance in the backscattering hemisphere.

Fig. 2 to 5, and others not shown here, demonstrate the ability of the airborne POLDER instrument to measure the reflectance directional signature of surface targets. The main advantage of airborne remote sensing, when compared to surface measurements, for the evaluation of directional signature is its ability to sample surfaces whose typical length scale is larger than one meter. For instance, the directional signature of a vineyard or an orchard is not accessible from the surface. Another advantage is the capability of assessing the directional signature and their variations at the regional scale.

4 SPATIAL EXTENSION OF ANGULAR SIGNATURE

In order to quantify the directional signature of the surface, we make use of a simple directional model. The reflectance is assumed to be a linear combination of an isotropic term, and two anisotropic functions derived from physical considerations (Roujean et al., 1992b):

$$R(\theta_s, \theta_v, \varphi) = k_0 + k_1 \ f_1(\theta_s, \theta_v, \varphi) + k_2 \ f_2(\theta_s, \theta_v, \varphi) \qquad (2)$$

The values k_0, k_1 and k_2, are determined by a best linear fit over the measurements. Since both functions are normalized so that they are 0 for θ_s=θ_v=0, k_0 is the reflectance when both the sun is and the sensor are at zenith. Thus, k_0 is a reflectance corrected for angular effects, i.e. *normalized*. Similarly, k_1/k_0 and k_2/k_0 provide a quantitative estimate of the surface directional signature.

We performed the linear fit for each wavelength and each pixel independently. The procedure yields the three k_i and the correlation between the measurements and the model. Fig. 6 is a map of the k_0 for both 550 and 850 nm. The covered area is the same as in Fig. 1. The Rhone river can clearly be identified as a wide band of low reflectance at both wavelengths. Values are as expected and the spatial structure can be correlated with a land use map that was made during the measurement campaign. This result confirms that several directional measurements can be used to provide a single normalized value.

k_1/k_0 and k_2/k_0 provide a quantitative estimate of the directional signature. A major objective is to relate these coefficients to surface characteristics. Although their maps do show some structure, it has proved difficult to correlate their values to surface coverage indicated by the land use map.

The correlation between the model and the measurements is very satisfactory as shown in Fig. 7. This figure provides a cumulative histogram of the correlation over the study area for 550, 650 and 850 nm. There is a

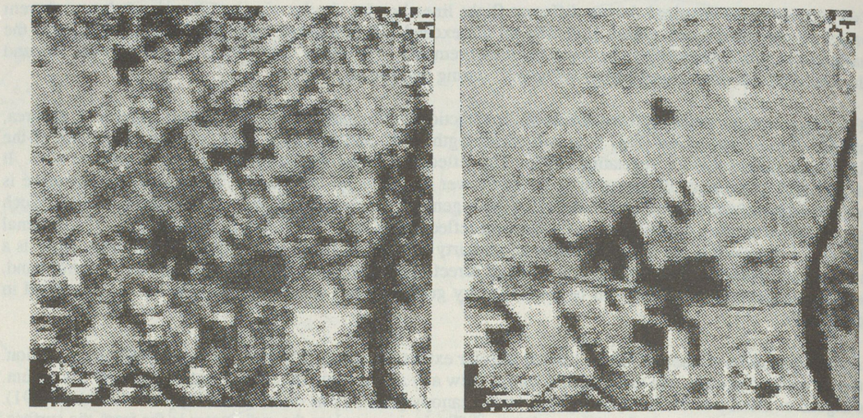

Figure 6: Map of the normalized reflectance, k_0, over the study area. The left figure is for 550 nm with a reflectance that increases from 0 to 20 % from black to white. The lower figure is for 850 nm and the same grey level scale is from 10 to 50%.

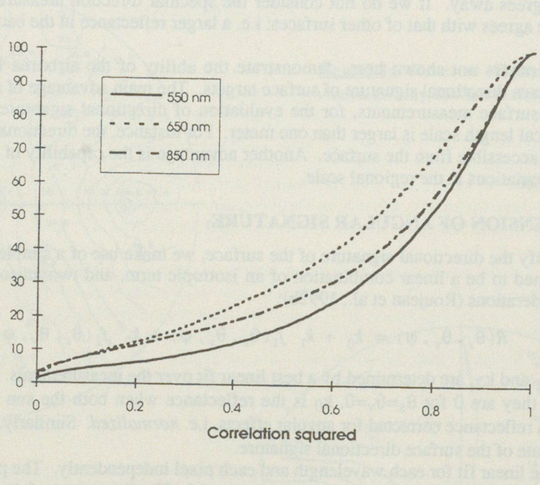

Figure 7: Cumulative histogram of the measurement-model correlation coefficient for 550 nm, 650 nm and 850 nm. A given point on the curve indicates the percentage of pixels of the 10 x 10 km area with a square of the correlation coefficient lower than its abcissae.

squared correlation coefficient, R^2, larger than 0.8 for 50% of the area and smaller than 0.5 for about 20% of it at 550 and 850 nm. The results are somewhat less good at 650 nm, may be because the level of reflectance is lower at this wavelength and therefore more sensitive to noise. A map of the correlation coefficient (not shown) allows us to identify the pixels for which the directional model is not satisfactory (i.e. when the correlation is lower than 0.5). Those correspond to i) river and canal, ii) rice paddies, and iii) pixels with few measurements (NE and SW corners of the study area). River, canals and rice paddies show a large specular reflection signal that is not accounted for in the functions f_1 and f_2. When the specular direction is disregarded, the model can reproduce the directional signature of the rice as it does for other canopies. On the other hand, the reflectance of water is mostly specular and its value in other directions is hardly distinguishable from noise. The pixels located in the NE and SW corners of the study area are relatively far from all flight lines. Thus, few observations correspond to these points and they are all acquired for large viewing angles. The measurements show little variation hardly distinguishable from noise, which yields a small correlation.

The results presented in this section show our ability to derive from POLDER directional measurements a reflectance corrected for angular effects. This correction is of uppermost importance for a comparison of measurements acquired from different instruments with various geometry. Similarly, a "normalized" reflectance is useful if we want to derive empirical relationships that yield physical surface parameters from the reflectances. We acknowledge that we have not shown that our corrected reflectance is better than a simple averaging of the measurements. Although the procedure is reasonable, it may introduce additional noise which could actually deteriorate the data quality. We must therefore imagine a procedure to compare the usefulness of our corrected reflectance k_0, with either a reflectance derived from the same set of data but with a simpler procedure (simple averaging of all directional measurements, for example), or the reflectance that would be acquired with a traditional scanner (only one directional measurement). The difficulty for such a validation is the lack of direct validation dataset: we do not have surface reflectance measurements for the *normalized* geometry, especially at the spatial scale used here. Thus, indirect methods are needed.

One method to validate our normalisation procedure is to compare the k_0 obtained for a given surface target from various datasets of directional measurements. Our data is well suited for this procedure since we can compare, for instance, the outcome of various flight line measurements. We can also compare the k0 obtained from all measurements in the forward scattering hemisphere, with those from the backscattering hemisphere.

Another validation procedure could make use of the land use map which was elaborated by INRA, from surface survey, during the campaign. One can determine, for each of the surface type classes, the variability (standard deviation or another statistical indicator) of the k_0, and that of the reflectance derived with other procedures. A small variability intra-class when compared to the distance between each class, indicates that surface types can be discriminated from the parameter. A smaller variability intra class indicates a better parameter, and the method which derives the k_0 can be quantitatively compared to other normalisation procedures.

Finally, we can also make use of POLDER measurements acquired, over the same area, during other days. Similar flight plans have been used and the processing described above can be repeated. The spectral normalised reflectance and angular signatures obtained from the various flight measurements can be compared since we can assume little variability of the surface during the campaign time period. This validation procedure evaluates, in particular, the atmospheric correction since the various flights have been performed with various optical thicknesses.

These validation procedures will be performed in the near future and their results will be presented in a forthcoming paper.

5 DISCUSSION AND CONCLUSION

The study presented in this paper shows that meaningful reflectance directional signatures are accessible from airborne POLDER measurements. A key point is the confidence we have in the measurements. Our data accuracy is limited mostly by two factors: i) spatial registration of the measurements and ii) atmospheric effects on the reflectance.

Many effects contribute to the misregistration of our measurements, including the GPS uncertainty, a bad timing between the GPS and the measurements, and an uncertainty on the radiometer optical axis. A misregistration induces discontinuities in the derived reflectance angular signature that can easily be identified. This effect is particularly troublesome for very heterogeneous (at the measurement scale) landscapes such as those in the northern part of our study area. The quality of the surface targets directional signatures which we studied in detail, and the high correlation between the model and the measurements shows that the data are relatively well registered. We believe misregistration is responsible for the lower correlation found in the northern part of our study area.

The measurements we used for the retrieval of surface directional signature have been selected for their relatively low atmospheric optical thickness. Atmospheric measurements have been acquired at the same time as POLDER flight and we have therefore a high confidence in our atmospheric correction. Uncertainty remains since aerosol optical thickness measurements are sensitive to the *total* optical thickness whereas atmospheric correction needs that *below* the aircraft. Besides, atmospheric effects induce a directional signature that is hardly distinguishable from the surface signature. Thus, a small signal from the atmosphere may remain in our data but the main signature is generated by the surface.

The method we used in this study to process POLDER data matches in part that which is envisioned for the opertational processing of spaceborne POLDER data. Our results give confidence in the soundness of the method, especialy since spaceborne measurement registration will have a much better relative accuracy. The POLDER instrument on ADEOS will provide a global estimate of surface reflectance directional signatures at resolution 6x6 km. With the method described above, POLDER measurements yield a reflectance corrected for angular effects, which is well suited for a quantitative monitoring of the surface.

ACCNOWLEDGMENTS

The POLDER instrument has been designed, built, serviced and operated by the Laboratoire d'Optique Atmosphérique (LOA), Lille, France, with a sponsorship from the Centre National d'Etudes Spatiales (CNES). We acknowledge the work of many individuals from this laboratory who participated to the "La Crau-91" experiment and made this study possible, and in particular J.Y. Balois, C. Devaux, M. Herman and C. Verwaerde. The help from several personel from CNES and INRA was also appreciated. The POLDER airborne campaign, placed under the responsibility of A. Podaire, was made possible by a sponsorship of the Programme National de Télédétection Spatiale (PNTS).

REFERENCES

Baret F., Leprieur C., Jacquemoud S., Carrere V., Gu X.F., Steven M.D., Vanderbilt V.C., Hanocq J.F., Ustin S., Rondeaux G., Daughtry L., Biehl L., Pettigrew R., Modro D., Horoyan H., Sarto T., Despontin C., and Razafindraibe H.; 1992: The 1991 AVIRIS/POLDER experiment in Camargue, france. In R. O. Green (Ed.), Third annual JPL Airborne Geoscience workshop., 92-14,75-77. Pasadena, California, USA: JPL.

Bréon, F.M. and P.Y. Deschamps; 1993: Optical and Physical parameter retrieval from POLDER measurements over the ocean using an analytical model. *Rem. Sens. Enviro.*; **43**, 193-209.

Coulson, K.L., and D.W. Reynolds; 1968: The spectral reflectance of natural surfaces. *J. App. Met.*, **10**, 1285.

Deschamps, P.Y., F.M. Bréon, M. Herman, M. Leroy, A. Podaire, A. Bricaud, J.C. Buriez, J.L. Deuzé, G. Sèze, 1993: The POLDER mission: Instrument characteristics and scientific objectives. *IEEE Trans. Geosc. Rem. Sens.;* in press.

Deuzé, J.L., F.M. Bréon, P.Y Deschamps, M. Herman, A. Podaire, and J.L. Roujean : Analysis of the POLDER Airborne Instrument Observations over Land Surfaces. *Rem. Sens. Enviro*., **45**, 137-154.

Duggin M.J., D. Piwinski, V. Whitehead, and G, Ryland, 1982, 'Evaluation of NOAA-AVHRR data for crop assessment', *Applied Optics*, **21**, 1873-1875.

Goel N. S. and D. W. Deering, 1985, 'Evaluation of a canopy reflectance model for LAI estimation through its inversion', *IEEE Trans. Geosc. Rem. Sens.;* GE-23, 674-684.

Gutman. G.G., 1987, 'The derivation of vegetation indices from AVHRR data', *Int. J. Rem. Sens.*, 8, 1235-1243.

Holben B. N., 1986. 'Characteristics of maximum-value composite images from temporal AVHRR data', *Int. J. Rem. Sens.*, vol. 7, 1417-1434.

Jupp D. L. B. and A. H. Strahler, 1991, 'A hot-spot model for leaf canopies', *Rem. Sens. Enviro.*, 38, 193-210.

Kimes D.S., 1983, 'Dynamics of directional reflectance factor distribution for vegetation canopies', *Applied Optics*, **22**, 1364-1372.

Kimes D.S., W.W. Newcomb, C.J. Tucker, I.S. Zonneveld, W. Van Wijngaarden, J. de Leeuw, and G.F. Epema, 1985, Directional reflectance factor distributions for cover types of Northern Africa, *Rem. Sens. Enviro.*, 18, 1-19.

Kimes D.S., W.W. Newcomb, R.F. Nelson, and J.B. Schutt; 1986: Directional reflectance distributions of a hardwood and a pine forest canopy, *IEEE Trans. Geosc. Rem. Sens.*, GE-24, 281-293.

Kriebel, K.T., 1978, Measured spectral directional reflection properties for four vegetated surfaces. *Applied Optics*, **17**, 253-259.

Otterman, J. and G.H. Weiss, 1984: Reflection from a field of randomly located vertical protrusions. *Applied Optics*, **23**, 12,1931-1936.

Pinty, B., M.M. Verstraete, and R.E. Dickinson, 1989, A physical model for predicting bidirectional reflectances over bare soil. *Rem. Sens. Enviro*., **27**, 273-288.

Roujean J. L., M. Leroy, A. Podaire, and P. Y. Deschamps, 1992a: Evidence of surface reflectance bidirectional effects from a NOAA/AVHRR multi-temporal data set, *Int. J. Rem. Sens.*, **13**, 685-698.

Roujean, J.L., M. Leroy, P.Y. Deschamps; 1992b: A bidirectional reflectance model of the Earth surface for the correction of remote sensing data. *J. Geophys. Res.*, **97**, 20455-20468.

Verhoef, 1985, Earth observation modeling based on layer scattering matrices, *Rem. Sens. Enviro*, **17**, 165-178.

Verstraete, M.M., B. Pinty and R.E. Dickinson, 1990, A physical model for predicting the bidirectional reflectance of vegetation canopies. 1. Theory. *J. Geoph. Res.*, **95**, D8, 11755-11765.